IAC-22-B1.IP.x72860

Analysis and design of future multiple satellite formation flying L-band missions in low Earth orbit

Francesca Scala[a]*, Camilla Colombo[b], Berthyl Duesmann[c], Manuel Martin-Neira[d]

[a] *Department of Aerospace Science and Technology, Politecnico di Milano, Via La Masa 34, 20156 Milano, Italy,* francesca1.scala@polimi.it
[b] *Department of Aerospace Science and Technology, Politecnico di Milano, Via La Masa 34, 20156 Milano, Italy,* camilla.colombo@polimi.it
[c] *Earth Observation Projects Department, European Space Research & Technology Centre (ESA), Keplerlaan 1, Postbus 299, 2200 AG Noordwijk, The Netherlands,* Berthyl.Duesmann@esa.int
[d] *Electrical Department, European Space Research & Technology Centre (ESA), Keplerlaan 1, Postbus 299, 2200 AG Noordwijk, The Netherlands,* Manuel.Martin-Neira@esa.int
* Corresponding Author

Abstract

In the context of future L-band missions, the need to improve the spatial resolution with respect to the ESA's Soil Moisture and Ocean Salinity (SMOS) mission should be addressed for future follow-on studies with a range of applications over land and oceans. Since November 2009, SMOS has been producing global maps of soil moisture and sea surface salinity with an average resolution of 40 km, which play a key role in the improvement of meteorological and climate monitoring and prediction. Future mission studies should address the need for a resolution down to 1-10 km. Such improvement in the resolution of a radiometer can only be obtained by increasing the aperture size with either a bigger satellite or a formation of multiple platforms working as a distributed node of a sensor of a network. In this paper, the latter strategy is envisioned as a potential way to improve spatial resolution. Starting from the outcomes of the Formation Flying L-band Aperture Synthesis (FFLAS) study concept, proposed by the European Space Agency, this paper addresses novel formation geometries, considering multiple satellites acting as distributed radiometer sensors. Specifically, up to six identical platforms are envisioned to improve spatial resolution. Considering the scientific mission requirements of the L-band interferometer, tight and rigid formation geometries are studied for Low Earth Orbit application. First, possible configurations are analysed in the local orbital frame to minimise the effect of orbital perturbations and to balance the fuel consumption among the platforms. To fulfil the requirements of the L-band interferometer, the requirement in the typical distance among the satellites is in the order of meters, which poses a great challenge in terms of control strategies and safe mode definition. The maintenance of a rigid formation to perform aperture synthesis is achieved by continuous control thrust with electric propulsion engines. The relative dynamics are propagated in a high-fidelity environment, including the main perturbing effects of the LEO region. As demonstrated by the FFLAS study, control accuracies in the centimetre order can be reached thanks to the design of a robust control strategy. At the same time, guidance and navigation strategies are presented to assess the feasibility of the study, in terms of both navigation and control accuracies.

Keywords: SMOS, L-band radiometer, formation flying, relative motion

1. Introduction

Nowadays, Earth observation missions provide vital information to improve monitoring and assessing the status of the natural and man-made environment. Remote sensing satellites, carrying observation instruments, gather data for several everyday services: from climate change monitoring and hydrometeorological processes to agricultural practices, ocean wealth and circulation and many others [1].

In this context, the passive L-band radiometry in Low Earth Orbit (LEO) could be used to collect data to measure the impacts on terrain, as soil moisture, and on ocean, with sea surface salinity maps, sea ice thickness and global winds maps. Moreover, L-band radiometry could also improve the knowledge of the galaxy map, Sun radiation and the total electron content in the ionosphere. One of the most relevant missions in L-band is the ESA's Soil Moisture and Ocean Salinity (SMOS) mission, launched in 2009, and still operational today. The spacecraft mounts the Microwave Imaging Radiometer with Aperture Synthesis (MIRAS) payload, able to gain a spatial resolution of about 40 km [2].

Given the importance of the data gathered by SMOS, this paper focus on the design of possible follow-on missions. The analyses presented in this paper are based on the outcome of the Formation Flying L-band Aperture Synthesis (FFLAS) study [3] [4]. FFLAS was carried out by Airbus Defence and Space and Politecnico di Milano under an ESA's contract. The study demonstrated the feasibility of a three-hexagonal spacecraft flying in

formation to improve spatial resolution. SMOS was able to provide global maps with a spatial resolution of about 40 km as a single satellite, and formation flying is seen as a means to improve spatial resolution with combined interferometry. Specifically, the FFLAS study demonstrated that the three-satellite formation, as in Fig. 1, can achieve a spatial resolution of about 10 km, and formation flying is a path enabling high spatial resolution for future L-band passive observations [5].

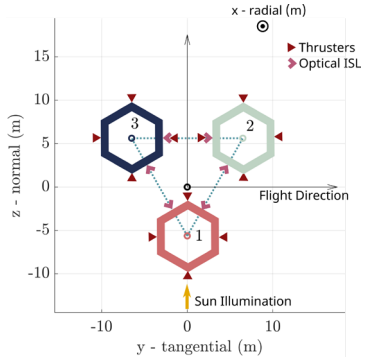

Fig. 1. Nominal configuration of the three-satellite formation in the FFLAS study [4].

Starting from the FFLAS outcomes, this work proposes a future development of the study, increasing to six the number of spacecraft in the formation. The motivation behind this new study is connected to multiple aspects:

- Passing from single to multiple spacecraft, the same spatial resolution can be achieved by smaller platforms, reducing the cost and mass of the mission.
- Smaller platforms can be injected into orbit by smaller launchers, reducing again the cost of the mission.
- In this paper, the increase from three to six spacecraft allows a reduction in both the diameter and mass of the spacecraft of factor two.

This manuscript aims at proposing two different formation flying geometries for L-band interferometry, analysing the feasibility from the delta-v and the control accuracy point of view during formation maintenance. The work proposes a novelty approach to combine the design of the formation geometry with the performance of the payload, and at the same time, the control accuracy is led by the requirements of the L-band interferometer. The selected scenarios are tested in a high-fidelity simulator, which includes the main orbital perturbations in LEO. The simulator is used to test the control accuracy during the formation maintenance, and the considerations about the safety of the formation.

Section 2 briefly presents the L-band radiometer performances depending on the shape of the antenna and the spatial resolution of different scenarios. Then, section 3 describes the design and selection of the formation flying configurations with six satellites, including a discussion on the possibility to design a fuel balancing strategy for formation maintenance. Finally, section 4 presents the assessment of the performance for the two-formation geometry selected, providing the delta-v budget over one day of simulation.

2. Remote sensing with spacecraft formation

After the outcomes of the SMOS, the main research question connected to the L-band observation was to find a new approach to improve the spatial resolution, without increasing the size of the platform. In fact, the outer envelope of SMOS spacecraft was about 8 m, and it was feasible with deployable antennas. Moreover, the possibility to change the shape of the antenna was investigated as well [5] [6].

2.1 L-band array geometry

In the FFLAS study, the shape of the antenna array was modified from the Y-shaped of the SMOS spacecraft to the hexagonal one.

Several studies demonstrated that different shapes of the antenna array led to different performances of the synthetic beam [6]. This can be roughly evaluated from the synthetic beam response of the antenna. Starting from the theory in [7] [8], the coverage and the synthetic beam response are reported for the Y-shaped and hexagonal-shaped antenna.

The side-lobes of the synthetic beam response are good indicators of the resolution of the array. Lower is the value of the side lobe in comparison to the main lobe of the response, better is the spatial resolution.

For the SMOS satellite, the side lobes levels are around -13 dB. Fig. 2 represents the geometry, the coverage, and the synthetic beam response for the Y-shaped antenna. The data and assumptions for this analysis are consistent with the work in [6].

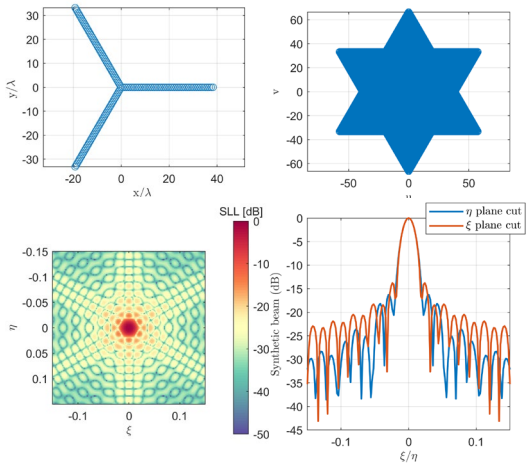

Fig. 2. Geometry (top left), coverage (top right), and synthetic beam (bottom) for the Y-shaped antenna.

Passing to the hexagonal shape, with similar parameters, as in [6], the side lobes level significantly reduces to -28 dB. Fig. 3 represents the geometry, the coverage, and the synthetic beam response for the Y-shaped antenna.

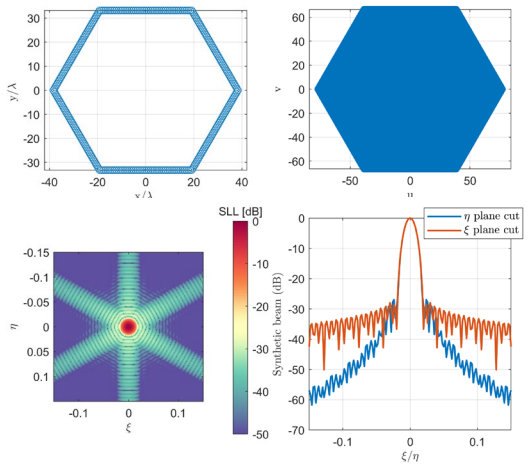

Fig. 3. Geometry (top left), coverage (top right), and synthetic beam (bottom) for the hexagonal-shaped antenna.

2.2 *L-band interferometry with formation flying*

The main drawback of the representation in Fig. 3 is the big size of the antenna array and, consequently, of the platform. Therefore, the possibility to combine multiple spacecraft with a similar coverage figure, as in Fig. 3 top right, is envisioned to reduce the platform dimensions.

- *FFLAS study: three satellite formation*

The FFLAS study in [3] [4] demonstrated the possibility to combine three L-band antennas, working as nodes of a network of sensors, providing a similar coverage of Fig. 3. The results of the combined interferometry are shown in Fig. 4. The side lobe levels are around -20 dB, confirming quite an improvement in comparison with SMOS spacecraft.

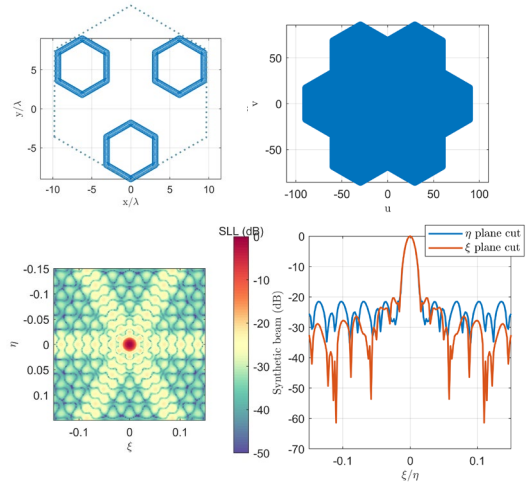

Fig. 4. Geometry (top left), coverage (top right), and synthetic beam (bottom) for 3-satellites formation.

- *Six satellite formation*

In FFLAS, the outer diameter of the spacecraft is around 8 m. In the direction of reducing, even more, the dimension of the spacecraft, this work proposes the possibility to use six spacecraft flying in formation to obtain a similar side lobes level. This results in an outer diameter of the platform of about 4.5 m. The results of the combined interferometry with six spacecraft are shown in Fig. 5. The side lobe levels are around -19 dB, confirming a similar performance with FFLAS, and quite an improvement in comparison with SMOS spacecraft.

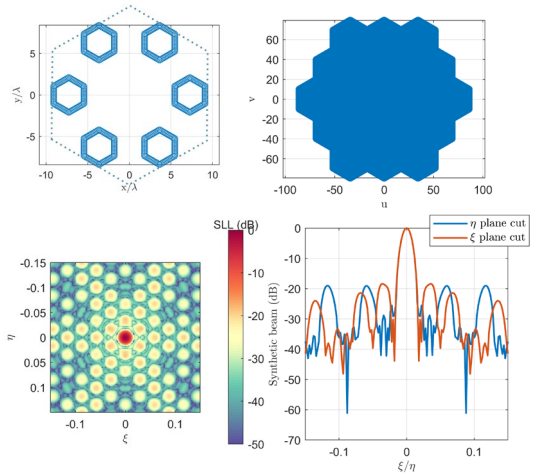

Fig. 5. Geometry (top left), coverage (top right), and synthetic beam (bottom) for 6-satellites formation.

2.3 *Considerations on the spatial resolution*

The graph in Fig. 6 compares the spatial resolution in both nadir and boresight for different cases and geometries, as in [5] [6].

A significant improvement is present passing from the single satellite to the formation flying concept. From the 40.6 km of SMOS, the three and six-satellite formation can achieve down to 10 km of spatial resolution in both directions. Moreover, exploiting the hexagonal antenna array, make the resolution symmetric in boresight and nadir, removing the unbalance in SMOS, where about 7 km difference was present.

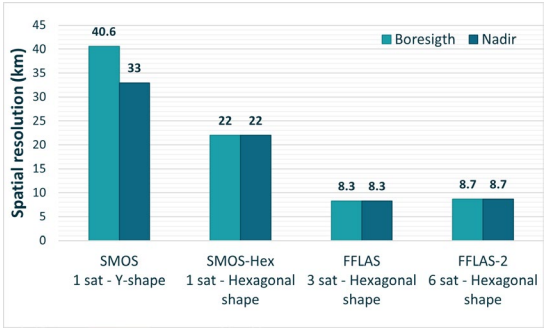

Fig. 6. Improvement in the spatial resolution changing the shape of the L-band array and increasing the number of spacecraft.

3. Design of formation geometries

This section describes the analyses performed to select the baseline formation with six satellites. First, the requirements coming from the payload poses significant constraints on the design of the formation geometry. Then, two strategies are proposed:

- Possibility to exploit natural solution of the relative motion
- Forced relative motion

The geometry of the relative motion is described in the radial-transversal-normal (RTN) orbital frame, also defined as the Hill Orbital Frame [9]. The RTN unit vector triad is defined as $\{x, y, z\}$, where x is aligned with the radial direction, pointing outward, z is aligned with the orbit momentum vector, and y to complete the right-hand coordinates system.

On the other hand, the relative dynamic is described in the relative orbital elements frame, as in [10]. Differently from the classical RTN representation, the ROEs allow a semi-analytical representation of the dynamical model, with a better insight into the relative motion.

3.2 Passive L-band payload requirements

The main requirements given by the L-band array are the following [3]:

Table 1. Payload requirements for the formation flying.

Planar geometry	The L-band arrays of different spacecraft shall belong to the same plane, called the Array Plane.
Tilt angle	The tilt angle δ of the array plane in the direction of motion should not exceed 32 degrees limit: $\delta < 32$ deg.
Array plane inclination	The inclination ϕ of the array plane around the transversal-normal plane of the relative reference system shall be smaller as possible $\phi < 10$ deg.
Relative distance	The relative distance among the platform in the formation shall be kept fixed, to allow a correct reconstruction of the combined synthetic beam.
Relative attitude	The relative distance among the platform in the formation shall be kept fixed, to allow a correct reconstruction of the combined synthetic beam.

3.3 Formation design parameters

From the requirements in Section 3.2, we defined the main design parameters for the selection of the formation geometry.

- Number of spacecraft: $n_{sat} = 6$
- Tilt angle of the array plane: δ
- Inclination angle of the array plane: ϕ
- Orientation of the formation in the array plane: γ

The angles ϕ, δ and γ are called respectively roll, pitch and yaw angles, as in Fig. 7.

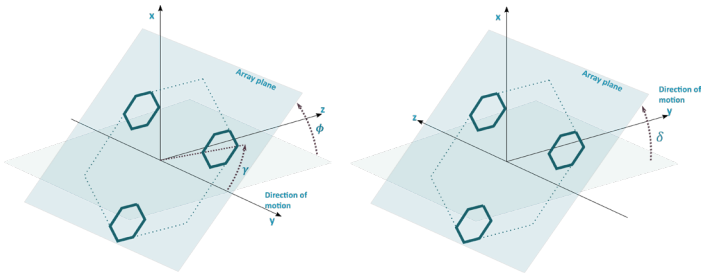

Fig. 7. Graphical representation of the design parameters (δ, ϕ, γ) in the radial-transversal-normal (x, y, z) plane of the relative motion.

The objective of the analysis is to present possible formation configurations and two possible scenarios are identified based on the inclination and tilt of the array plane: ϕ, δ can either be null ($\phi, \delta = 0$ deg) or not ($0 < \phi < 10$ deg and $0 < \delta < 32$ deg).

3.4 Case 1: Generic roll angle

The first scenario can be identified when the array plane is inclined over the transversal-normal direction. In this context, the unperturbed relative motion admits analytical solutions for a close orbit that respect the payload requirement of $\delta < 32$ deg, but not the inclination one: $\phi \not< 10$ deg. The analytical solution called general circular orbits (GCO) was already studied in the literature in several works [11] [12].

Given the amplitude of motion ρ_x, ρ_y and ρ_z, in the x, y and z direction respectively, and the phase angles α_x and α_y, the periodic relative motion can be expressed in the relative orbital elements frame, defined by $\{\delta a, \delta\lambda, \delta e_x, \delta e_y, \delta i_x, \delta i_y\}$:

$$\begin{cases} \delta a = 0 \\ \delta\lambda = \rho_y \\ \delta e_x = -\rho_x \sin\alpha_x \\ \delta e_y = -\rho_x \cos\alpha_x \\ \delta i_x = \rho_z \cos\alpha_z \\ \delta i_y = \rho_z \sin\alpha_z \end{cases} \quad (1)$$

The analytical solution of interest for this work is called the general circular orbit (GCO), obtained by imposing a circular motion of the deputies around the chief position. The parameters to set up the GCO are:

$$\rho_x = \frac{1}{\sqrt{3}}\rho, \quad \rho_y = 0, \quad \rho_z = \rho, \quad \alpha_x = \alpha_z = \alpha \quad (2)$$

The GCO is designed for six deputies, orbiting around a virtual chief spacecraft. The geometry of the solution is such that the inclination of the array plane is around 30 deg over the y, z plane of the relative frame.

The choice of this kind of orbit was driven by the following considerations:

- The use of a natural solution of the relative motion is a stable orbit, and the control action required for formation maintenance when

considering a perturbed environment is small (as demonstrated in section 3.6).

- The external perturbation similarly affects the six spacecraft, resulting in a balanced delta-v consumption for formation maintenance (see section 5.2.1).
- The stable nature of the analytical solution guarantees robust collision avoidance in case of failure of the control (see section 5.2.2). The external perturbations lead to an unsafe situation over one day period. Nevertheless, robust planning of the safe mode transition is essential for safe operations.

Fig. 8 represents the GCO trajectory for a six-satellite formation. The relative orbit was initialised with $\rho = 14.8$ m to reproduce a correct reconstruction of the L-band synthetic beam. The phase angle of each satellite is $[270 \quad 330 \quad 30 \quad 90 \quad 150 \quad 210]$ deg in order 1 to 6 respectively. The representation also shows the projection of the GCO over the x, y, and z planes, and the array plane inclination is computed from the projection of the GCO over the x, z plane.

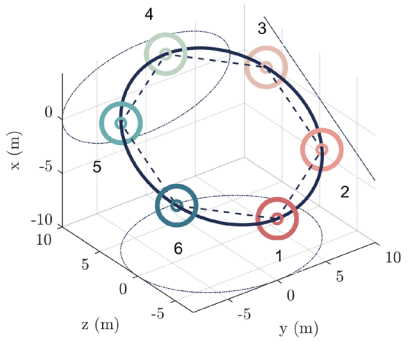

Fig. 8. Six satellite formation lying on a general circular orbit with $\rho = 14.8$ m.

3.5 *Case 2: Null roll-pitch angle*

A second scenario is identified when the array plane inclination is null: $\phi = 0$ deg. This results in an array plane orthogonal to the radial direction of the relative frame. The six satellites are placed in a hexagonal formation geometry, as shown in section 2.2. The dimension of the hexagon side is about 10.3 m to allow the correct payload interferometry reconstruction.

This second option initially considers the hexagonal formation centred in the origin of the relative frame (virtual chief position), and it requires a continuous forced motion to maintain the relative state of each spacecraft. The relative motion can be described in the relative orbital elements frame by the coordinates $\{\delta a, \delta\lambda, \delta e_x, \delta e_y, \delta i_x, \delta i_y\}$. This description provides a better insight into the time variation of the deputies' elements in comparison with the classical hill representation.

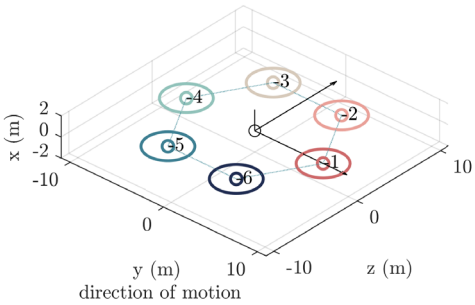

Fig. 9. Six satellites flying in a hexagonal formation, lying on the transversal-normal (y, z) plane.

Fig. 9 represents the hexagonal formation of the six spacecraft, centred on the origin of the reference system. The distance centre-to-centre between a couple of adjacent spacecraft is 10.3 m, and the platform diameter is about 4 m. This configuration was driven by the following considerations:

- To maintain a fixed geometry among the spacecraft in the y, z plane of the relative system, a forced motion is required since no analytical solution can be obtained for a natural motion.
- The continuous control required to maintain the formation poses some safety issues in case of a failure of one engine. An immediate transition to the safe mode configuration must be implemented to avoid any unsafe situations and possible collisions.
- The fuel consumption for formation maintenance is proportional to the absolute value of the out-of-plane coordinate z of each spacecraft.

3.6 *Propagation in the LEO perturbed environment*

The natural propagation in the LEO environment is performed to understand the effect of the main external disturbances. In this work, the effects of the gravitational potential and the atmospheric drag are considered:

- Gravitational model: the GRACE gravity model includes the effect up to the order and degree 6x6 [13].
- Atmospheric drag model: the NRLMSISE-00 model has been considered to include the seasonal variation effects [13].

The perturbing accelerations are added to the two-body problem as [13]:

$$\ddot{r} = -\frac{\mu}{r^3} r + a_{grav} + a_{drag} \tag{3}$$

Where r is the absolute state of the spacecraft, and μ is the Earth's gravitational constant. The gravitational acceleration a_{grav} is included in the spacecraft's absolute motion through the partial derivatives of the gravitational potential U:

$$U = \frac{\mu}{r}\sum_{l=2}^{\infty}\sum_{m=0}^{l}\left(\frac{R_{earth}}{r}\right)^{l} P_{l,m}[\sin(\phi_{gc_{sat}})] \{C_{l,m}\cos(m\,\lambda_{sat}) + S_{l,m}\sin(m\,\lambda_{sat})\} \quad (4)$$

Where R_{earth} is the mean radius of the Earth, $P_{l,m}$ are the associated Legendre functions, $\phi_{gc_{sat}}$ is the geocentric value of the latitude, λ_{sat} is the satellite longitude, and, finally, $C_{l,m}$ and $S_{l,m}$ are the zonal harmonics coefficients.

The aerodynamic drag is included in the absolute dynamics as a perturbing acceleration defined as:

$$a_D = -\frac{1}{2}\rho_a\, C_D \left(\frac{A}{M}\right) v_{rel}^2 \frac{v_{rel}}{|v_{rel}|} \quad (5)$$

Where ρ_a is the density of the atmosphere and it was computed with the NRLMSISE-00 model, C_D is the drag coefficient of the spacecraft, A is the spacecraft cross-sectional area, M is the spacecraft mass, and v_{rel} is the spacecraft velocity vector relative to the atmosphere. In this work, we considered $C_D = 2$, $A = 3$ m^2, and $M = 700$ kg.

From the high-fidelity propagation of the absolute motion, the relative dynamic is computed in the relative orbital elements system, to understand the natural motion of each formation configuration.

Case 1: Natural propagation in the GCO trajectory

Spacecraft 6 (see Fig. 8) was propagated in the perturbed environment over two days (corresponding to about 30 orbital periods). The propagation in the relative orbital elements is shown in Fig. 10. The graph represents a translational effect in the relative eccentricity vector $(\delta e_x, \delta e_y)$, in the y component of the relative inclination vector $a\delta i_y$ and in the relative argument of latitude $a\delta\lambda$. On the other hand, the relative semi-major axis $a\delta a$ and the x component of the relative inclination vector are subjected to oscillatory behaviour.

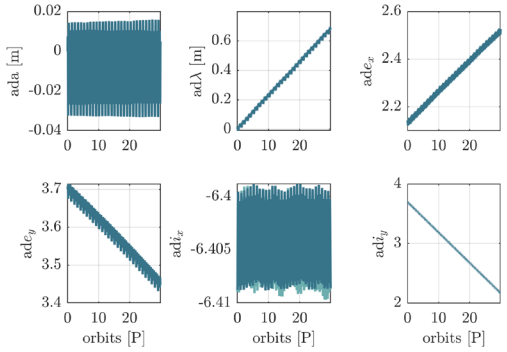

Fig. 10. Natural propagation of satellite 6 in the GCO configuration (in absence of control).

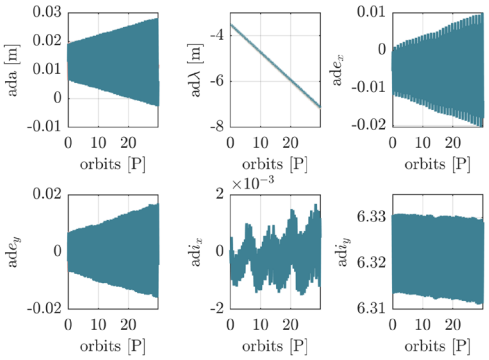

Fig. 11. Natural propagation of spacecraft 6 in the hexagonal formation geometry (in absence of control)

Case 2: Natural propagation in the hexagonal trajectory

The spacecraft 6 (see Fig. 9) was propagated in the perturbed environment over two days and the corresponding time evolution of the relative orbital elements is reported in Fig. 11. Both a translational and an oscillatory effect are present in most of the components of ROEs.

Comparing the dynamical behaviour in Fig. 11 with the propagation of the GCO case, we observe that most of the ROEs components are mostly affected by an oscillatory motion. This behaviour is divergent in time for the components $a\delta a$, $a\delta e_x$ and $a\delta e_y$.

For both the GCO and the planar cases, control is essential to maintain the formation geometry during the payload observation phase.

4. Guidance, control, and navigation strategy

The analysis performed in this work is based on the guidance, navigation, and control (GNC) simulator tool developed in previous work by Scala et al. [14].

The simulator aims to provide a design tool to assess the control and navigation performances of the relative motion of multiple satellites flying in formation. The main features of the simulator are:

- MATLAB/Simulink environment for the development and simulation of the absolute and relative propagator of the dynamics, the control strategy and navigation reconstruction.
- Inclusion in the dynamical propagator of main LEO perturbation (see section 3.6), as the gravitational potential and the atmospheric drag.
- Implementation of a low thrust continuous control in the closed-loop, based on the linear quadratic regulator.
- Absolute and relative navigation reconstruction based on the Global Navigation Satellite System (GNSS) sensors in single frequency.

4.1 Formation maintenance and control strategy

The formation maintenance for both cases 1 and 2 requires the definition of the reference trajectory to be followed by the on-board computer.

Case 1. The reference trajectory is computed by propagating the initial condition for the GCO in an unperturbed environment.

Case 2. In this case, the spacecraft shall be kept fixed in their initial relative position, therefore, the reference trajectory is defined by the initial state of each deputy.

In this paper, the control system implements a linear quadratic regulator approach in a closed-loop system. The control logic is defined as follows:

$$u = u_i - K\,(x - x_i) \tag{6}$$

Where u_i is the ideal control for the formation maintenance, K is the gain matrix, x is the actual relative state and x_i is the reference trajectory. The terms $(x - x_i)$ represents the feedback error for the control. The gain matrix K is computed by solving Riccati's equation of the LQR problem [14].

The ideal control profile is computed for both cases 1 and 2. For the *GCO case* the ideal control can be computed as in [15]:

$$\begin{cases} \ddot{x} = 0 \\ \ddot{y} = -\dfrac{1}{2}\rho_x(\dot{\omega} + \dot{\alpha}_x)\cos\left(\lambda + \alpha_x + \left(\dot{\lambda} + \dot{\alpha}_x\right)t\right) \\ \ddot{z} = -2\,n\,\dot{\alpha}_x\,\rho\sin\left(\lambda + \alpha_x + \left(\dot{\lambda} + \dot{\alpha}_x\right)t\right) + \\ \qquad 2\,\rho k \sin^2 i_c \cos\alpha_x \sin\lambda \end{cases} \tag{7}$$

Where $\dot{\alpha}_x$ is the phase angle rate due to the J2 effect, and $\dot{\lambda}$ is the precession rate of the argument of latitude. The parameter k introduces the dependence on the Earth's oblateness: $k = 1.5\,n\,J_2\left(\frac{R_{earth}}{a_c}\right)^2$. Finally, a_c and i_c are the semi-major axis and the inclination of the reference orbit.

For the *planar case* (case 2) a forced relative motion is imposed. To compute the ideal control effort required to maintain the formation rigid, the general solution of the unperturbed Hill-Clohessy-Wiltshire equations is considered [9]. Imposing that the relative position components x, y, z shall remain equal to the initial condition of the formation (x_0, y_0, z_0), we compute the acceleration components to maintain the formation rigid:

$$\begin{cases} \ddot{x} = -3\,n^2 x_0 \\ \ddot{y} = 0 \\ \ddot{z} = n^2 z_0 \end{cases} \tag{8}$$

Where n is the mean motion of the absolute orbit. In both cases 1 and 2, the ideal control is computed from the acceleration values $u_i = [\ddot{x}, \ddot{y}, \ddot{z}]$.

4.2 Relative navigation strategy

A decentralised approach is selected for autonomous navigation management, without mediation from a specific satellite [14]. Each spacecraft is supposed to have the same computational and data-handling capabilities. Consequently, it can elaborate its GNC algorithms autonomously, by exchanging GNSS data via the optical link among the platforms. The exchange of raw GNSS navigation data enables the reconstruction of the absolute and relative state of each satellite with respect to the virtual reference point, at each time instant.

The logic behind the data exchange among the satellite is the following:

- Each spacecraft receive its navigation data from the GNSS network and transmit it to the other satellites of the formation.
- Every spacecraft receives the navigation data from the other platforms and autonomously computes the absolute and relative state estimate in the relative frame centred on the virtual reference point.

5. Results

For both case 1 and case 2, the feasibility and the performance of the formation maintenance are tested with the GNC simulator. The analysis aims to identify:

- Control accuracy with a continuous control logic with a limitation in the thrust magnitude: $|T| < T_{max}$.
- Delta-v budget for a 1-day simulation period and the balancing of fuel consumption among the spacecraft.
- Safety considerations and implications for the safe mode design.

5.1 Reference orbit definition

This work considers as reference orbit the same Keplerian parameter of SMOS spacecraft. It was initialised on a Sun-Synchronous Orbit (SSO) at the mean altitude of 775 km. We consider an orbital cycle of 3 days, resulting in $14 + 1/3$ orbits per day; consequently, every 3 days, the spacecraft passes over the same geographical point on the ground.

Table 2 shows the Keplerian elements of the reference orbit in the Earth Mean Equator (EMEJ2000) reference frame.

Table 2. Keplerian elements of the reference orbit in the EMEJ2000 reference frame.

h_c (km)	e_c (-)	i_c (deg)	Ω_c (deg)	ω_c (deg)	M_c (deg)
775	0	98.51	270	0	0

5.2 Case 1: GCO formation

The first case analysed in this work is the formation of six satellites in the GCO configuration. The initial parameters of the simulation are reported in Table 3.

The simulation aims at analysing the feasibility of the formation maintenance over 1 day period in terms of:

- Delta-v budget and fuel consumption balancing among the spacecraft.
- On-board control accuracy on the relative state.

Finally, some considerations on the formation safety in case of failure are provided.

Table 3. Simulation parameters for the GCO formation.

Parameter	Value
Initial UTC time	21/03/2025 12:00:00
Simulation time	1 day
Step size	5 sec
Platform diameter	4.5 m
Atmospheric drag	yes
Gravity field	yes
Order n, degree m	6,6
GCO parameters	
ρ	7.4 m
α_x	[30 90 150 210 270 330]

5.2.1 GNC simulation

The first aspect analysed is the delta-v budget for formation maintenance. Continuous control is needed to counteract the external perturbations of the LEO environment.

The delta-v is evaluated in the radial-transversal-normal frame for each platform of the formation over one day period. We considered a three-axis thrust system for formation control. The results are shown in the left graph of Fig. 12. The analyses result in:

- An almost balanced delta-v budget among the six spacecraft in all directions, with a magnitude of the delta-v in every direction in the cm/s level.
- The most relevant term in the control must be provided in the radial direction, with a daily delta-v of about 0.38 cm/s.
- The control required in the normal direction is the less expensive, with a daily delta-v of about 0.08 cm/s.
- The magnitude of the delta-v in the transversal direction is around 0.25 cm/s

From this analysis, it results that the continuous control of the formation in the GCO configuration is not expensive, requiring a daily delta-v for formation maintenance smaller than 1 cm/s.

The second aspect of primary importance is the evaluation of the control performance. The LQR controller is used to provide the commanded thrust to the model of the low thrust engine, which introduces noises and delays in the command. These values are dependent on the engine selection. Moreover, a limitation on the thrust is imposed, and in this scenario, a maximum thrust of 1 mN was considered.

The control accuracy on the relative state of the spacecraft was evaluated considering the error between the actual relative state and the reference trajectory, at each time instant, as $e_{cntr} = |x - x_i|$. The results are reported in the central graph of Fig. 12, describing the control accuracy in the radial-transversal-normal direction. The error in the control in the three directions is below 1 cm accuracy, granting accurate formation maintenance.

5.2.2 Formation safety considerations

An important analysis must be done to understand the behaviour of the formation when a failure in the control is present. We consider the propagation with no control applied over one day period, considering as a safety threshold the platform diameter with a 40% margin.

The right graph of Fig. 12 shows the relative distance among the platform if no control is applied: the spacecraft remain in a safe configuration over one day of propagation.

Nevertheless, the divergent behaviour of the relative motion requires actions to guarantee a safe flight: the transition to the safe mode shall be implemented in a maximum one-day period.

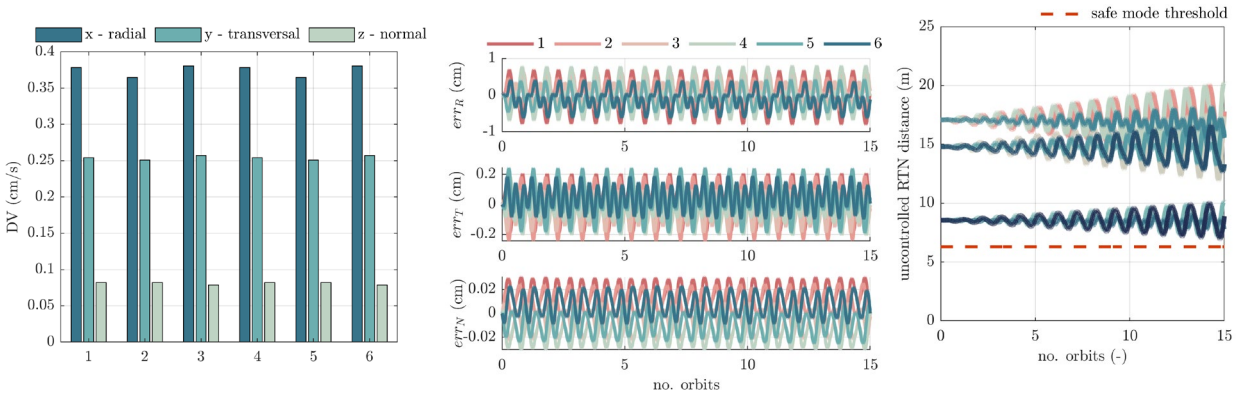

Fig. 12. Simulation results for the GCO formation: on the left the daily delta-v is reported in the RTN components, in the centre the control error, and on the right the distance among the spacecraft with no control applied.

5.2.3 *Final discussion*

Starting from the results in sections 5.2.1 and 5.2.2, the general circular orbit solution of the relative motion results in the following benefits:

- The external perturbations cause a small oscillation and translation of the relative trajectories in comparison to the nominal natural motion.
- A small daily delta-v effort is required to counteract external perturbation and is balanced among the spacecraft.
- The natural behaviour in case of a failure requires the safe mode to be implemented in a maximum of one day period.
- The violation of the inclination requirement (ϕ is not smaller than 10 deg), requires a future additional analysis to understand the payload behaviour and the possible losses in the performances (swath losses)

5.3 *Case 2: hexagonal formation*

The second case analysed in this work is the formation of six satellites in the hexagonal configuration. The initial parameters of the simulation are reported in Table 4. The simulation aims at analysing the feasibility of formation maintenance over 1 day period in terms of:

- Delta-v budget and fuel consumption balancing among the spacecraft.
- On-board control accuracy on the relative state.

Finally, some considerations on the formation safety in case of failure are provided.

Table 4. Simulation parameters for the GCO formation.

Parameter	Value
Initial UTC time	21/03/2025 12:00:00
Simulation time	1 day
Step size	5 sec
Platform diameter	4.5 m
Atmospheric drag	yes
Gravity field	yes
Order n, degree m	6,6
Hexagon shape	
Latus dimension	7.4 m

5.3.1 *Initial analysis for delta-v budget*

The first analysis was performed considering the hexagonal geometry of the formation as represented in Fig. 9. Since the effort for the formation maintenance is proportional to the relative position in the normal direction, the delta-v budget is not balanced among the spacecraft, as shown in Fig. 13:

- The fuel consumption is not symmetric, the relative motion is such that spacecraft 1 and 4 require only a small effort (around 0.5 cm/s) for counteracting the external perturbations since they lie on the direction of motion (y-axis).

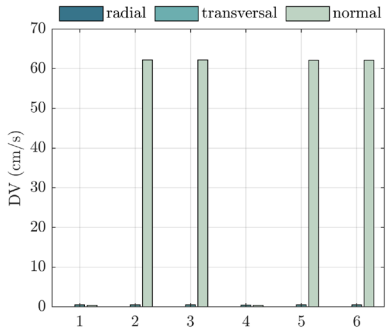

Fig. 13. Initial analysis for the daily delta-v budget considering the baseline hexagonal formation.

- On the other hand, spacecraft 2, 3, 5, and 6 require continuous control to counteract the natural behaviour of the relative motion as well as the external perturbations, resulting in a daily budget of about 60 cm/s.

The unbalance in the delta-v budget and the fuel consumption causes in time a difference in the mass of the spacecraft. This asymmetry may generate different effects due to the external perturbation on the relative motion and requires a non-symmetric design of the platform itself, for tanks and fuel mass dimensioning.

A fuel balance strategy is required to remove this effect.

5.3.2 *Fuel balance strategy*

Different approaches were investigated to achieve e delta-v balance among the spacecraft. The selected strategy consists of:

a. Step 1:

- The hexagonal geometry of Fig. 9 is initialised with a translation in the positive direction of the z-axis of the RTN frame.
- The magnitude of the translation is selected to bring the spacecraft 5 and 6 on the y axis (direction of motion): $\Delta z_{up} = 6.329$ m. This configuration is called "up formation", shown in Fig. 13.

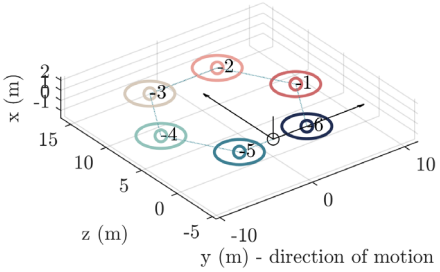

Fig. 14. Geometry of the "up formation" in RTN frame.

b. Step 2:

- The "up formation" is modified again with a translation in the z-axis direction.

- This new translation aims at placing spacecraft 2 and 3 on the y-axis (direction of motion).
- The magnitude of the translation with respect to the geometry in Fig. 9 is Δz_{down} = - 6.329 m. This second configuration is called "down formation" and it is shown in Fig. 15.

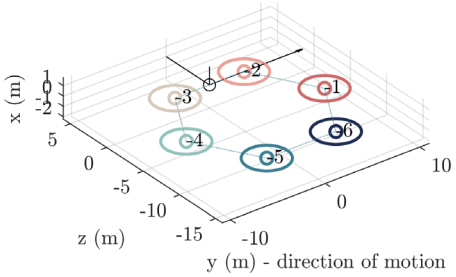

Fig. 15. Geometry of the "down formation" in RTN frame.

The main idea of the strategy is to alternate the "up" and "down" configurations to assess delta-v balance. For example, alternating 1 day in the "up" and one day in the "down" configuration, we evaluate the delta-v budget over two days period.

Fig. 16 shows the delta-v budget over one day period for the formation maintenance of the "up" and "down" configuration on the left and right graphs, respectively. As expected, the couple of spacecraft 2,3 and 5,6 requires a minimum control (< 1 cm/s) alternated to maximum control of about 120 cm/s. Combining the delta-v budget for one day in the "up" and one day in the "down" configuration, results in a balance of formation maintenance, as shown in Fig. 17. The result of the analysis shows a balance in the delta-v over two days among the spacecraft.

Extending this concept to an operation phase of a mission, we consider 1 year of scientific operations, where the following strategy can be implemented:

- 6 months in the "up formation"
- Formation reconfiguration
- 6 months in the "down formation"

In this way, the fuel consumption is balanced among the platform, and a symmetric design of the spacecraft can be implemented: the implementation of 6 identical platforms can reduce the overall cost of the mission.

5.3.3 GNC simulation

After the analyses of the delta-v balance, the performance of the control during the formation maintenance is assessed. The results for the error in the control on the relative position are shown in Fig. 18. Differently from the previous GCO case, the analysis was performed limiting the maximum available thrust to 25 mN.

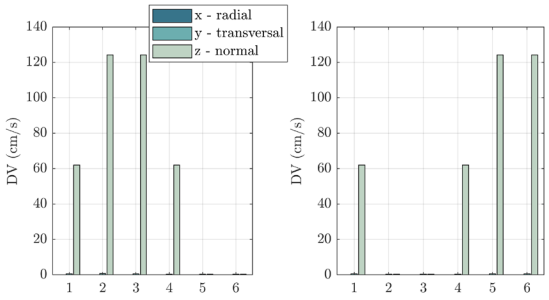

Fig. 16. Daily delta-v budget for the up (left) and down (right) formation.

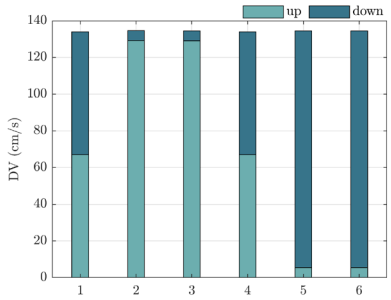

Fig. 17. Delta-v budget over two days period by alternating one day in "up" and one day in the "down" configuration.

The GNC simulation shows that control in the cm order is achievable with the LQR controller. The error in the relative state is more significant in the transversal direction, where the control error in the position is limited to 15 cm. In the other directions, the accuracy is better, and it is below 4 cm and 0.2 cm in the radial and normal directions, respectively.

5.3.4 Formation safety considerations

As in section 5.2.2, we carry out an analysis to understand the behaviour of the formation when a failure in the control is present. We consider the propagation with no control applied over one orbital period, considering as a safety threshold the platform diameter with a 40% margin, as in the dot red line in Fig. 18 right. It shows how the spacecraft crosses the safety threshold in less than one orbital period, if no control is applied, making collision avoidance critical.

This behaviour requires a robust and autonomous on-board control system for the instantaneous transition to a safe mode. The main constraint shall be the actual distance among spacecraft at each time instant, and this value shall be monitored constantly during the mission. If any failure is detected, an immediate response shall be designed for a safe continuation of the formation.

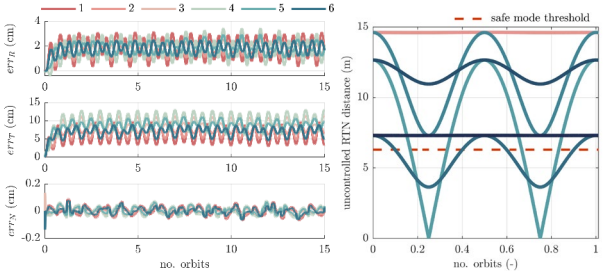

Fig. 18. Control accuracy of the relative state (left) and relative distance among the spacecraft in case of failure in the control (right).

6. Conclusions

To conclude, the two approaches presented in this work have different advantages and disadvantages. The first one, which considers the spacecraft on a GCO relative trajectory, is more advantageous for the formation maintenance and safety procedure, requiring a smaller delta-v for maintaining the formation (below 1 cm/s daily) and ensuring a 1-day margin to implement the safe mode transition. On the other hand, it has an inclined array plane, resulting in possible worst performances from the L-band radiometer point of view. This is a key aspect to be analysed in a future work.

The second case, considering a hexagonal geometry of the formation, maintains the plane of the array orthogonal to the radial direction, ensuring the best outcomes from the payload interferometry. On the other hand, it results in a more expensive formation maintenance strategy, with a daily delta-v budget of about 60 cm/s. Moreover, the safety and failure considerations are more critical, requiring an autonomous transition to safe mode in less than one orbital period.

Finally, this study demonstrated the benefits of exploiting different formation geometries for Earth observation purposes. One of the main advantages from point of view of passive L-band radiometry is the possibility to achieve the same or better spatial resolution with smaller spacecraft. This improves the cost-benefit of the mission and increases redundancy in case of failure. Moreover, more accurate data (down to 10 km of spatial resolution) for soil moisture and ocean salinity. Considering the guidance, navigation, and control techniques, we demonstrated that the current low-thrust technology is capable to provide control for formation keeping and that the control of close formation (in the meter range) can be kept in the millimetre to centimetre range. Therefore, an on-board autonomous algorithm is required for manoeuvre and formation keeping and safe mode transition.

This study is in the direction of selecting and assessing possible scenarios for realising SMOS follow-on missions. The analysis gives confidence in both navigation knowledge and control accuracy, ensuring the necessary robustness to avoid collisions.

Acknowledgements

The main author, Francesca Scala, was awarded the ESA-ISEB sponsorship by the European Space Agency in collaboration with the International Space Education Board to participate in the International Astrodynamics Conference (IAC22).

The authors want to acknowledge the collaboration with Dr Miguel Piera, from Airbus Defence and Space, leading the contract to develop the FFLAS study (founded by the European Space Agency, Contract No. 4000128576/19). The view expressed in this paper can in no way be taken to reflect the official opinion of the European Space Agency.

The work was founded by the European Research Council (ERC) under the European Unions Horizon 2020 research and innovation program (grant agreement No. 679086 COMPASS).

References

[1] M. Martin-Neira, B. Duesmann, M. Piera, A. Zurita, F. Scala e C. Colombo, «Formation flying L-band aperture synthesis mission concept.,» in *2022 IEEE International Geoscience and Remote Sensing Symposium (IGARSS 2022)*, Kuala Lumpur, Malaysia, 17-22 July 2022.

[2] K. D. McMullan, M. A. Brown, M. Martin-Neira, W. Rits, S. Ekholm, J. Marti and J. Lemanczyk, "SMOS: The payload," *IEEE Transactions on Geoscience and Remote Sensing 46,* p. 594–605, 2008.

[3] M. Onoda and O. R. Young, "Satellite Earth observations and their impact on society and policy," *Springer Nature,* 2017.

[4] F. Scala, G. Gaias, C. Colombo e M. Martin-Neira, «Formation flying l-band aperture synthesis: Design challenges and innovative formation architecture concept.,» in *71st International Astronautical Congress (IAC 2020)*, Virtual Conference, 12-14 October 2020.

[5] M. Martin-Neira, M. Suess, N. Karafolas, P. Piironen, F. Deborgies, A. Catalan, R. Vilaseca e J. Montero, «Technology developments for an advanced l-band radiometer mission,» in *2020 IEEE International Geoscience and Remote Sensing Symposium (IGARSS 2020)*, Virtual Symposium, 26 September to 2 October 2020.

[6] A. Zurita, I. Corbella, M. Martin-Neira, M. A. Plaza, F. Torres e J. Benito, «Towards a SMOS Operational Mission: SMOSOps-Hexagonal,» *IEEE Journal of Selected Topics in Applied Earth Observations and Remote Sensing,* vol. 6, n. 3, June 2013.

[7] A. K. Sugihara El Maghraby, A. Grubisic, C. Colombo e A. Tatnall, «A Novel Interferometric Microwave Radiometer Concept Using Satellite Formation Flight for Geostationary Atmospheric Sounding,» *IEEE Transaction on Geoscience and Remote Sensing,* vol. 56, n. 6, pp. 3487-3498, June 2018.

[8] C. Erbeia, *Modelling and control of interferometer formation flying mission in low Earth orbit,* Master Thesis at Politecnico di Milano, Milan, 2022.

[9] W. H. Clohessy e R. S. Wiltshire, «Terminal guidance system for satellite rendezvous,» *Journal of the Aerospace Sciences,* vol. 27, n. 9, pp. 653-658, 1960.

[10] S. D'Amico, *Autonomous formation flying in low earth orbit,* PhD Thesis, Technical University of Delft, Delft, The Netherlands, 2010.

[11] F. Scala, C. Colombo e M. Martin-Neira, «Design of natural collision-free trajectories for the mission extension phase of a remote sensing formation flying mission,» in *72nd International Astronautical Congress (IAC 2021)*, Dubai, UAE, 25-29 October 2021.

[12] S. R. Vadali, P. Sengupta, H. Yan e K. T. Alfriend, «Fundamental frequencies of satellite relative motion and control of formations,» *Journal of Guidance, Control, and Dynamics,* vol. 31, n. 5, pp. 1239-1248, 2008.

[13] D. A. Vallado, Fundamentals of astrodynamics and applications, vol. 12, Springer Science & Business Media, 2001.

[14] F. Scala, C. Colombo e M. Martin-Neira, «A decentralised approach for formation flying reconfiguration and maintenance using GNSS-based navigation,» in *AIAA Scitech 2022 Forum*, San Diego, CA, 23-27 January 2022.

[15] M. D'Errico e G. Fasano, Relative trajectory design. In: Distributed space missions for earth system monitoring, vol. 31, S. T. Library, New York, NY: Springer, 2013.